Pol. J. Environ. Stud. Vol. XX, No. X (XXXX), 1-13
DOI: *10.15244/pjoes/220217* ONLINE PUBLICATION DATE: 2026-07-30

Original Research

Mechanisms of Hydrochemical Evolution and Water Quality Evaluation in Shallow Groundwater of Xutuan Coal District, Anhui, China: A Multi-Method Approach

Jie Chen[1], Jiying Xu[1,3]*, Hongbao Dai[2], Haitao Zhang[1], Jie Ma[1], Yan Guo[1]

[1]School of Resources and Civil Engineering, Suzhou University, Suzhou, 234000, Anhui, China
[2]School of Environment and Surveying and Mapping Engineering, Suzhou University, Suzhou, 234000, Anhui, China
[3]Coal Industry Engineering Research Center for Exploration and Early Warning of Mine Water Disaster, Anhui University of Science and Technology, 232000, Huainan, Anhui, China

Received: 06 February 2026
Accepted: 31 March 2026

Abstract

This study investigates the hydrochemical characteristics of the shallow phreatic aquifer in the Xutuan coal mining area, Anhui, China, based on 20 collected water samples. A comprehensive analysis was conducted using techniques such as Piper trilinear plots, ionic ratios, Principal Component Analysis, and Entropy Weighted Water Quality Index (EWQI). The results show that the groundwater pH ranges from 0.05 to 8.89 (mean 5.08), indicating weak acidity; TDS varies from 96.09 to 1397.46 mg/L (mean 278.58 mg/L), classifying it as freshwater. The dominant cations are Na^+ and K^+ (mean 1834.08 mg/L), and the dominant anion is HCO_3^- (mean 4792.08 mg/L). The main hydrochemical facies is SO_4^{2-} HCO_3^--Na^+ K^+. Analysis of ionic composition and Gibbs diagrams reveals that the chemical evolution of groundwater is primarily influenced by water-rock interactions, including evaporative concentration, silicate weathering, and cation exchange processes. The EWQI assessment indicates that 85% of the samples meet Class II or III water quality standards (EWQI range: 38.5-120.4). While overall groundwater quality is acceptable, the quality in the local third aquifer layer is comparatively inferior, necessitating increased monitoring efforts. This study provides a scientific basis for groundwater environmental protection and sustainable water resource management, contributing to the long-term management of groundwater in coal mining areas.

Keywords: shallow groundwater, hydrochemical characteristics, Entropy Weight Water Quality Index (EWQI), coal mining area, water-rock interaction

*e-mail: jiyingxu1986@163.com
Tel.: +86-158-0557-4977
0000-0001-6709-3262

Introduction

Groundwater, as a crucial water resource, is of significant importance for fields such as water resource management, environmental protection, and geological engineering due to the distribution and evolution patterns of its chemical constituents [1]. Especially in the coal-resource-abundant areas of northern China, the hydrogeochemical features of groundwater systems are crucial for ensuring drinking water safety and agricultural water supply, while also acting as a vital portal to uncover mechanisms of water-rock interaction and water quality evolution [2].

With the acceleration of industrialization, particularly coal resource extraction, the groundwater environment in mining areas faces a series of potential impacts, including water level decline, water quality pollution, and ecological degradation [3]. Since its commissioning in 2004, with the increase in mining depth at the Xutuan Coal Mine, the phreatic aquifer water may be contaminated by the discharge of mine water and coal waste accumulation, thereby affecting groundwater quality. Furthermore, the decline in groundwater levels caused by coal mining may also trigger environmental issues such as land subsidence. Consequently, investigating the hydrochemical features of the shallow groundwater in this region is crucial for pinpointing contamination origins and evaluating the potential for sustainable water resource use.

Existing hydrochemical and water quality assessment methods have limitations in studying the phreatic aquifer in complex coal mining areas, urgently requiring the deep integration of internationally common techniques with China's unique hydrogeological conditions for targeted regional research. Methodologically, cluster and correlation analyses [4] have been used for hydrochemical evolution analysis, but a single method is insufficient to support systematic research on the phreatic aquifer. International research, however, focuses on innovations in mineral dissolution kinetics and hydrogeochemical modeling, such as using multivariate statistics [5] to analyze the synergistic effects of Himalayan glacial meltwater and rock weathering, or the Gibbs diagram method [6] to clarify the dominant role of evaporative concentration in the Dunhuang Basin. In the field of water quality assessment, fuzzy mathematics has gradually gained prominence due to its adaptability to multi-index nonlinear problems, and cluster optimization models [7] have also been used to identify mine water inrush sources. Nevertheless, international research largely centers on natural hydrological systems, with inadequate focus on tectonically complicated coal mining regions, and the suitability of existing models for China's distinctive hydrogeological context requires significant improvement, highlighting the need for a deeper fusion of regional studies and worldwide methods [8].

In terms of water quality assessment, conventional approaches frequently depend on the Single Factor Index Method [9] stipulated in the “Standard for Groundwater Quality” (GB/T 14848-2017) [10], which has difficulty representing the integrated water quality condition resulting from the collaborative action of numerous parameters. Recently, the Entropy-Weighted Water Quality Index (EWQI) [11], benefiting from its objective weighting that minimizes subjective bias, has been increasingly utilized for the integrated assessment of groundwater quality in mining regions. It facilitates quantitative categorization of water quality levels and the detection of spatial variations, offering scientific support for water resource management.

However, systematic research is still lacking on the hydrochemical characteristics and water quality evolution mechanisms of the phreatic aquifer groundwater in typical coal mining areas of the Huaibei Plain, particularly in the Xutuan region. Existing findings mostly focus on deep aquifers or the discrimination of mine water inrush sources, paying insufficient attention to the hydrochemical response processes of shallow groundwater under mining disturbance, and a technical pathway for water quality assessment based on multi-method coupling has not yet been established. Therefore, this study takes 20 sets of phreatic aquifer groundwater samples from the Xutuan coal mining area as the research subject. The novelty of this study lies in the first comprehensive application of Piper diagrams, ionic ratios, PCA, and EWQI to the shallow groundwater of Xutuan, revealing the combined influence of evaporation and rock weathering under mining impacts, and quantitatively evaluating water quality with an emphasis on anthropogenic disturbances.

Impact of Dry and Wet Conditions: The study used mean values of hydrochemical parameters collected during a single sampling campaign. However, dry and wet seasons can significantly affect groundwater chemistry through dilution or concentration effects. In the Xutuan area, the Beifei River is seasonal, and precipitation varies considerably between years. During wet periods, increased recharge may dilute ion concentrations, potentially improving water quality; during dry periods, evaporative concentration could elevate TDS and specific ions. The observed data represent an average condition, but long-term monitoring would be necessary to capture seasonal and interannual variability. Future studies should consider temporal sampling to assess the dynamic response of groundwater chemistry to climatic fluctuations.

Materials and Methods

Study Area Overview

Located in Mengcheng County, Anhui Province, the Xutuan Coal Mine falls under the administrative jurisdiction of Xutuan Town, Mengcheng County, Bozhou City, and lies in the central Huaibei Plain (Fig. 1). The central point of the mine is roughly 37

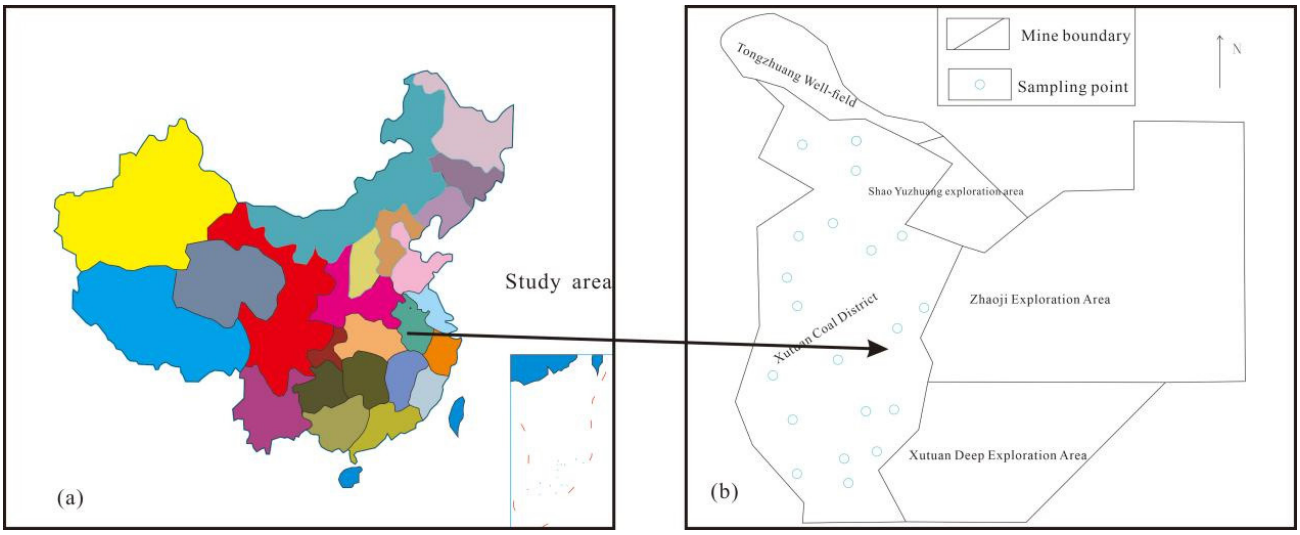

Fig. 1. Overview of the study area

km to the northeast of Suzhou City and some 28 km to the southwest of the Mengcheng County seat. The geographic coordinates are between 116°40′10″E and 116°44′41″E, and between 33°21′14″N and 33°27′35″N. This region features flat topography, where the northern part is marginally higher than the southern part. Surface elevations vary from +20.70 m to +28.46 m, averaging +25.43 m. Within the mining area, artificial canals crisscross, villages are densely distributed, and the Beifei River flows through the southern part of the mine. It is a tributary of the Huai River and is a seasonal river.

The study area is underlain by Quaternary unconsolidated sediments. The shallow phreatic aquifer, which is the focus of this study, is primarily composed of fine sand and silt. Its thickness ranges from 10 to 25 m, and its burial depth is 2-8 m below the surface. The aquifer is mainly recharged by atmospheric precipitation and lateral inflow from the seasonal Beifei River, and discharges through evaporation and artificial extraction. Regionally, a multi-layer aquifer system exists, with the phreatic aquifer underlain by the first, second, and third confined aquifers, separated by aquitards of clay and silty clay. The coal seams are situated within and below these confined aquifers, with the third confined aquifer being the closest to the mining operations. This hydrogeological setting makes the shallow aquifer potentially susceptible to both natural weathering processes and anthropogenic influences from coal mining activities.

Sample Collection, Processing, and Testing

In this study, a total of 20 sets of phreatic aquifer water samples were collected from the research area. Before sampling, the sampling buckets were rinsed three times with deionized water, and subsequently flushed three times with the water to be sampled at the collection point. After collection, the samples were delivered to the laboratory within 24 hours, vacuum-filtered through 0.45 μm membrane filters, and then stored in a refrigerator at 4°C for subsequent analysis.

The pH and total dissolved solids (TDS) of the water samples were measured using a portable OHAUS instrument. Measurements for sodium (Na^+), potassium (K^+), calcium (Ca^{2+}), and magnesium (Mg^{2+}) were conducted via an ISC-600 model ion chromatography system, wherein 1.3 mL of methanesulfonic acid was added to a 1000 mL volumetric flask to prepare the cationic eluent. The contents of chloride (Cl^-) and sulfate (SO_4^{2-}) anions were analyzed by an ICS-900 ion chromatograph, utilizing ultrapure water for elution. The hardness and bicarbonate (HCO_3^-) concentration were measured using acid-base titration methods. Before testing all samples, instrument stability was checked with standard reference materials, and parallel samples were run to ensure that the relative deviation of the parallel determinations remained within 5%.

Water Quality Assessment and Treatment Methods

Selection of Evaluation Indicators

The extant Standard for Groundwater Quality (GB/T 14848-2017) [8] of China constitutes a fundamental reference for evaluating groundwater quality. Groundwater quality is precisely categorized into five classes within this standard, considering the prevailing groundwater quality conditions in China, human health-based criteria, protection goals for groundwater quality, and stringent quality standards for potable, industrial, and agricultural water.

The selection of water quality evaluation indicators follows the principles of measurability, comparability, and sensitivity. Based on the water quality conditions within the study area, total dissolved solids, chloride, sodium, total hardness, pH, and sulfate were chosen as the primary impact indicators for assessment in the study area. In this context, the sodium value corresponds to

the total content of the sodium ion (Na^+) and potassium ion (K^+) indicators.

Principal Component Analysis (PCA)

Relying on the dimensionality reduction concept, Principal Component Analysis (PCA) [12] condenses multi-dimensional data by reducing its dimensionality, consolidates numerous intricate factors into several principal components, and interprets pollution conditions through the information represented by these components, finding extensive application in water quality analysis and assessment. By screening interrelated factors within the sample data, it identifies the primary environmental pollution influencing factors, groups factors belonging to the same component into one principal component. Each independent principal component encompasses most of the information from the original data, thereby simplifying the problem and enabling a scientific analysis of the pollution characteristics of groundwater in the study area.

Entropy Weight Water Quality Index (EWQI)

The Entropy Weighted Water Quality Index (EWQI) determines the weight of each indicator through entropy calculation, transforming a large amount of monitoring data into an objective value reflecting groundwater quality status and eliminating the influence of human factors in the calculation process. Its calculation steps are as follows:

1) Establish a matrix using the raw data as the foundation.

2) Perform standardization on the original data. Employing the range standardization method, the original data are normalized to eliminate scale discrepancies between different indicators, adjusting the data to a [0,1] interval. Initially, classify each indicator as a positive, negative, or interval type indicator. For this research, TDS, SO_4^{2-}, Cl^-, and Na^+ are identified as negative indicators, pH as an interval indicator, with no positive indicators present. Following this, apply formulae to transform the negative indicators into a positive direction and to normalize the interval indicators (with X_o representing the optimum value for the indicator). The specific calculation formulae are provided below.

$$\text{Negative Indicator } Y_{ij} = \frac{(X_{ij})\max - X_{ij}}{(X_{ij})\max - (X_{ij})\min} \quad (1)$$

$$\text{Interval Indicator } Y_{ij} = 1 - \frac{|X_{ij} - X_0|}{|X_{ij} - X_0|} \quad (2)$$

3) The standardized data for all indicators fall within the 0~1 range. To mitigate the impact of zero values and similar anomalies on the determination of weights, the entire dataset is offset by 0.0001 according to the following formula, after which the offset data are normalized.

$$Y_{ij} = Y_{ij} + 0.0001 \quad (3)$$

4) Normalization Processing.

$$P_{ij} = \frac{Y_{ij}}{\sum_{i=1}^{n} Y_{ij}} \quad (4)$$

5) Calculation of Information Entropy.

$$e_j = -\frac{1}{\ln m} \sum_{i=1}^{m} P_{ij} \cdot \ln P_{ij} \quad (5)$$

6) Determination of Entropy-based Weights.

$$\omega_j = \frac{1 - e}{\sum_{j=1}^{n} (1 - e_j)} \quad (6)$$

7) Quantitative Classification of Indicators. This step involves computation using the measured concentration (C_j) of each monitoring parameter and its respective threshold value (S_j), which is adopted from the Class III water quality standard limits for the parameters as defined in 'Standard for Groundwater Quality' (GB/T 14848-2017).

$$q_j = \frac{C_j}{S_j} \times 100 \quad (7)$$

8) Computation of EWQI and Classification of Water Quality. The calculated EWQI values are used to classify water quality into five categories [34]: Class I-II signifies good quality, Class III indicates moderate quality, Class IV corresponds to poor quality, and Class V represents very poor quality.

$$\text{EWQI} = \sum_{j=1}^{n} (\omega j \cdot \text{qj}) \quad (8)$$

Consequently, the derived EWQI intervals <25, 25~50, 50~100, 100~150, and ≥150 are respectively indicative of Class I, Class II, Class III, Class IV, and Class V groundwater quality.

Data Analysis Method

To explore the hydrochemical properties of the principal ions within the aquifer, this research utilizes mathematical statistics and Piper trilinear diagrams. Meanwhile, the formation mechanisms governing the

Table 1. Statistical Characteristics of Hydrochemical Indicators of Loose Layer Water in Xutuan Coal District.

Statistical item	$Na^+ + K^+$	Ca^{2+}	Mg^{2+}	Cl^-	SO_4^{2-}	HCO_3^-	TDS	pH
Unit	mg/L	mg/L	mg/L	mg/L	mg/L	mg/L	mg/L	/
Minimum	1040.12	170.14	151.15	104.1	298.13	1385.15	196.09	0.05
Maximum	6567.94	1067.74	760.59	514.04	3620.15	47097.07	1397.46	8.89
Average Value	1834.08	437.18	329.13	160.23	1369.57	4792.98	278.58	5.08
Standard Deviation	1137.08	278.2	166.13	102.02	687.97	9726.64	257.47	4.45
Coefficient of Variation	0.62	0.64	0.5	0.64	0.5	2.03	0.92	0.88

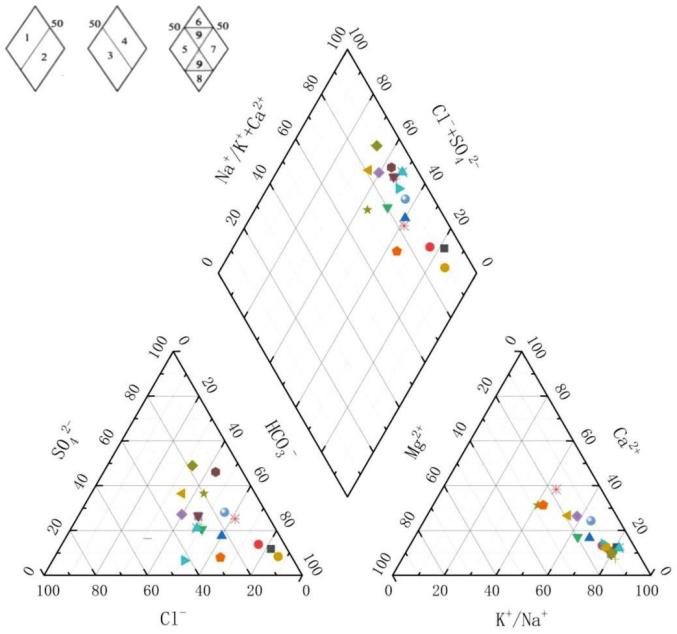

Fig. 2. Piper diagram of the phreatic groundwater samples from Xutuan Coal District.

chemical constituents of sandstone fracture water are analyzed using Gibbs diagrams and ion ratio analysis. Descriptive statistics were performed using Excel, whereas the creation of Piper diagrams, Gibbs diagrams, and ion ratio analysis diagrams was performed utilizing Origin2024 and CorelDRAW applications.

Results and Discussion

Hydrochemical Characteristics

The statistical results of the average values for major ion concentrations, TDS, and pH of the phreatic aquifer water samples from the Xutuan Coal District are presented in Table 1.

The data presented in Table 1 show that the pH values vary between 5.08 and 8.89, with a mean concentration of 5.08, suggesting the water body is, on average, mildly acidic. However, the range indicates both acidic and alkaline conditions. Total Dissolved Solids (TDS) concentrations fall within 96.09 to 1397.46 mg/L, with a mean value of 278.58 mg/L for the samples, which classifies the groundwater as freshwater based on the lower numerical range [13]. The average mass concentrations of cations are in the order: Na^+ and K^+ (1834.08 mg/L) > Ca^{2+} (437.18 mg/L) > Mg^{2+} (329.13 mg/L), indicating that Na^+ and K^+ are the dominant cations. The mass concentration of Ca^{2+} ranges from 170.136 to 1067.736 mg/L, while that of Mg^{2+} ranges from 151.145 to 760.59 mg/L. Anions follow this sequence based on average mass concentration: bicarbonate HCO_3^- (4792.98 mg/L) > sulfate $S0_4^{2-}$ (1574.86 mg/L) > Cl^- (1369.57 mg/L), indicating that bicarbonate is the dominant anion in the groundwater samples.

In assessing data variability, the coefficient of variation, calculated as the standard deviation divided by the mean, quantifies the dispersion of data points around the average [14]. Elevated coefficients of variation for groundwater indicators suggest significant instability in their hydrochemical makeup, thereby offering insights into the diverse processes of groundwater chemistry. In the aquifer of the Xutuan Coal District, TDS exhibits a coefficient of variation between 0.5 and 0.9,

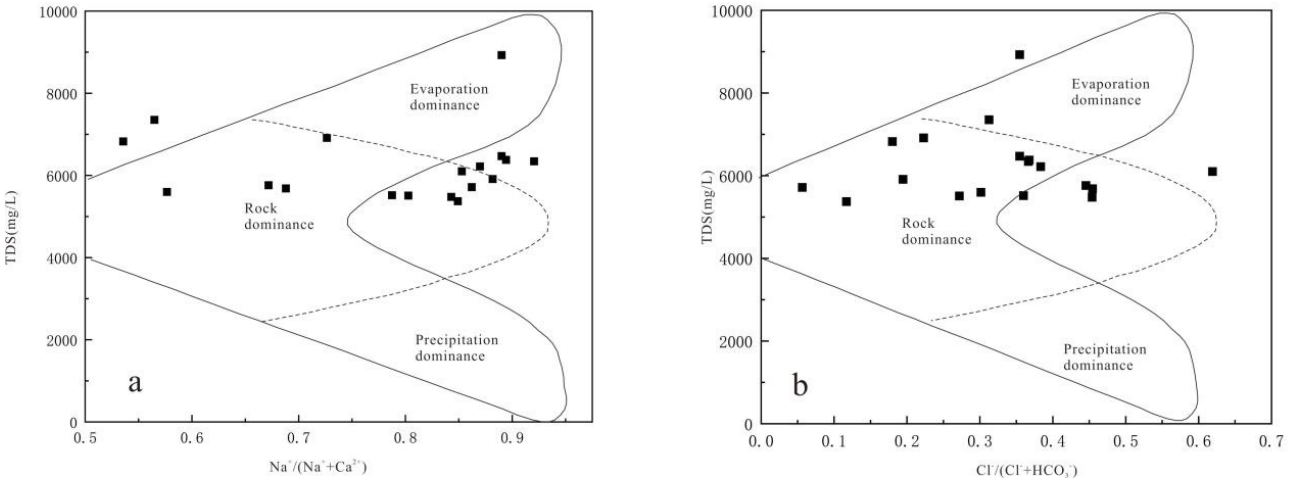

Fig. 3. Gibbs plot of the study area.

which denotes moderate variability for these indicators [15]. With a coefficient of variation of 0.88, pH shows pronounced spatial heterogeneity [16]. Only HCO_3^- exhibits a coefficient of variation exceeding 1, indicating that its concentration in the phreatic aquifer water is unstable and susceptible to changes in environmental factors [17].

The Piper trilinear diagram is a graph commonly used in hydrochemical analysis, aiding in the understanding and comparison of water sample chemical compositions and facilitating analysis of hydrochemical facies [18]. Fig. 2 displays the Piper diagram constructed for the phreatic water samples collected from the Xutuan Coal District.

Analysis of Fig. 2 reveals that in the phreatic aquifer water samples, alkali metal ions (Na^+, K^+) constitute over 80% of the total cations, significantly surpassing alkaline earth metal ions Ca^{2+}, Mg^{2+} and thus dominating the cation composition; the proportions of SO_4^{2-} and HCO_3^- are higher than that of Cl^-; the primary hydrochemical facies is SO_4^{2-}·HCO_3^-- Na^++K^+ type, while concentrations of Ca^{2+}, Mg^{2+}, and Cl^- are generally low, with elevated Cl^- levels observed only in a few samples. As presented in Fig. 2a), all samples are plotted in diamond field 2, which signifies a hydrochemical property characterized by a predominance of alkali metals over alkaline earth metals; the hydrochemical signature for the majority of samples is one where strong acid anions outweigh weak acid anions, whereas a minority of samples exhibit a signature where weak acid anions are more prevalent; in Fig. 2c), most water samples are located in diamond field 7, indicating that their hydrochemical character is defined by non-carbonate alkali hardness exceeding 50%; consequently, these samples are primarily composed of alkali metal ions and strong acids. A very small number of samples lie in field 8, signifying a hydrochemical character where carbonate alkali hardness exceeds 50%, and thus these samples are mainly constituted by alkaline earth metal ions and weak acids.

Hydrolithic Interaction

The Gibbs diagram is capable of revealing the dominant factors controlling hydrochemical processes, which aids in investigating the interplay between aqueous chemical composition and climatic or geological features [19]. In the Gibbs diagram, the mechanisms controlling hydrochemical processes are divided into three main domains: evaporation concentration, rock weathering, and atmospheric precipitation. The Gibbs diagram analysis of the water samples collected in the study region is shown in Fig. 3. Fig. 3a), depicting the relationship between TDS content and the $Na^+/(Na^+ + Ca^{2+})$ ratio, shows that TDS values range from approximately 2000 to 10000 mg/L. The data points are widely distributed across both the evaporation dominance and rock dominance fields, with a notable number of samples falling within or near the rock weathering domain. Similarly, Fig. 3b) (TDS vs. $Cl^-/(Cl^- + HCO_3^-)$) indicates a mixed influence, with samples spanning from precipitation-dominated to evaporation-dominated zones. This suggests that the chemical evolution of groundwater in the study area is governed by a combination of evaporation concentration and rock weathering processes, with atmospheric precipitation playing a minor role in certain samples.

Ion Ratio Analysis

Analyzing ion concentration ratios in groundwater aids in investigating its chemical composition and associated hydrogeochemical issues [20]. Diagrams illustrating specific ratios are presented in Fig. 4.

The Na^+/Cl^- molar ratio of 1 resulting from halite dissolution indicates that the groundwater chemistry is primarily formed by halite weathering and dissolution [21]; a ratio exceeding 1 suggests that Na^+ may have additional sources, such as the dissolution of other sodium salts.

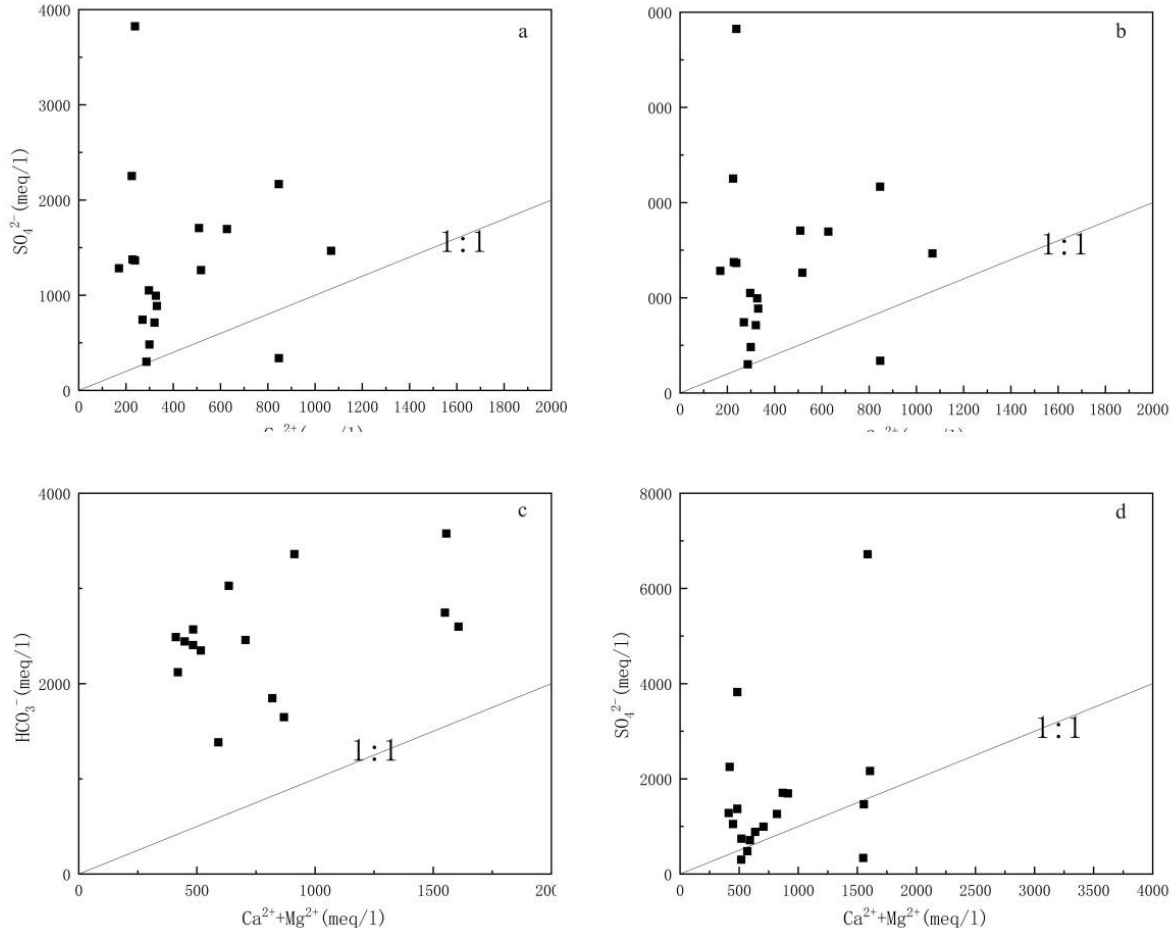

Fig. 4. Ion ratio results in water samples.

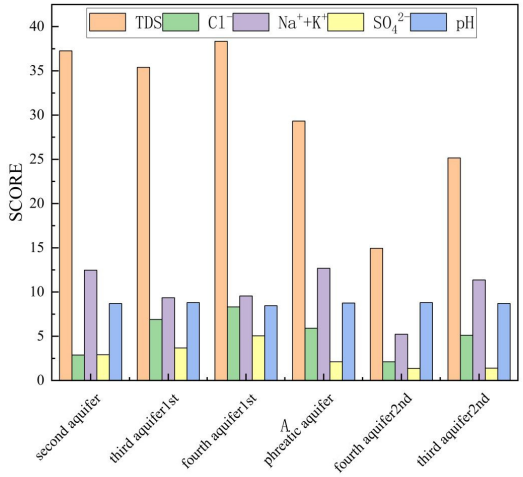

Fig. 5. Results of the evaluation index selection method.

As depicted in Fig. 4a), Na^+/Cl^- ratios in the phreatic water samples are all less than 1, which suggests Na^+ originates from sources beyond halite dissolution [22], possibly including silicate weathering or cation exchange processes in the aquifer [23] that lead to an enrichment of Na^+ relative to Cl^-.

The Ca^{2+}/SO_4^{2-} molar ratio of 1 in groundwater indicates that Ca^{2+} is primarily sourced from the dissolution of carbonate and sulfate minerals [24]. In Fig. 4b), the Ca^{2+}/SO_4^{2-} ratios of the phreatic aquifer water samples fluctuate around 1, indicating a relatively low Ca^{2+} content compared to SO_4^{2-}. This may be attributed to several factors: limited sources of Mg^{2+} in the

Table 2. Results of evaluation index selection method.

Aquifer	TDS	Cl^-	Na^++K^+	SO_4^{2-}	pH
Unit	meq/l	meq/l	meq/l	meq/l	/
Second aquifer	37.26	2.88	12.47	2.91	8.7
Third aquifer	35.4	6.9	9.35	3.67	8.8
Fourth aquifer1st	38.34	8.32	9.55	5.05	8.45
Phreatic aquifer	29.33	5.9	12.68	2.11	8.76
Fourth aquifer2nd	14.94	2.11	5.23	1.37	8.8
Third aquifer2nd	25.16	5.1	11.36	1.39	8.7

phreatic aquifer, oxidation of S^{2-} in the strata leading to increased SO_4^{2-} content [25], and weathering of silicate minerals in the coal measures contributing to elevated SO_4^{2-} levels [26]. The $(Ca^{2+} + Mg^{2+})/HCO_3^-$ molar ratio of 1 in groundwater suggests that Ca^{2+} and Mg^{2+} in the water are primarily derived from carbonate dissolution [27]. The water samples from this study show that in Fig. 4c), the contents of Ca^{2+} and Mg^{2+} are significantly lower than that of HCO_3^-, which further confirms the contribution of silicate weathering in the aquifer [28].

Since sulfate mineral dissolution constitutes an important ion source in groundwater, the $(Ca^{2+}+Mg^{2+})/SO_4^{2-}$ ratio is commonly employed to study the origins of Ca^{2+}, Mg^{2+}, and SO_4^{2-} [29]. In Fig. 4d), the majority of samples are positioned above the $(Mg^{2+})/SO_4^{2-} = 1$ baseline, suggesting that the dominant sources of SO_4^{2-} extend beyond mere sulfate mineral dissolution to incorporate additional contributions [30]. Combining the geological background of the Xutuan coal district, the coal-bearing strata contain pyrite and other sulfide minerals; coal mining activities expose these minerals to oxidation, releasing SO_4^{2-} into the groundwater. This anthropogenic influence, together with natural silicate weathering, explains the elevated SO_4^{2-} and the deviation of ion ratios from simple mineral dissolution trends.

Synthesizing the ionic ratio analyses, the ions in the phreatic water predominantly originate from carbonate and sulfate dissolution, coupled with silicate weathering.

Water Quality Evaluation

Assessment Parameters

As presented in Table 2, using the criteria selection method grounded in the "Standard for Groundwater Quality" (GB/T 14848-2017), the Total Dissolved Solids (TDS) for all samples are well under 1000 mg/L, placing them in the category of excellent freshwater (Class I or II). Concentrations of both Cl^- and SO_4^{2-} are substantially below 250 mg/L, corresponding to superior water quality. The sum of Na^+ and K^+ concentrations is under

Table 3. Principal component analysis results.

Aquifer	PC1 score	PC2 score	PC3 score	Water Quality Characteristics
Fourth aquifer	-2.15	-1.23	0.45	low mineralization, soft water
Third aquifer3rd	-1.98	-0.89	-0.32	low mineralization, extremely soft water
Second aquifer3rd	-1.45	1.02	-0.78	low mineralization, medium hardness
Third aquifer4th	-1.23	0.45	1.02	Low-mineralized, calcareous water
Phreatic aquifer	-0.78	-0.56	0.34	low mineralization, soft water
Third aquifer2nd	0.23	0.89	-0.45	moderate mineralization
Third aquifer1st	0.45	0.78	-0.23	moderate mineralization
Fourth aquifer3rd	0.78	-0.34	0.89	moderate mineralization, soft water
Fourth aquifer1st	1.02	-0.23	-0.56	higher mineralization
Second aquifer1st	1.23	0.34	0.78	higher mineralization, moderate hardness
Fourth aquifer2nd	1.45	-0.45	-0.34	high salinity, hypersalinity
Fourth aquifer4th	1.78	0.23	0.23	highly mineralized, sodium-rich water
Second aquifer2nd	1.98	0.56	-0.12	high mineralization, medium hardness

Table 4. Results of Entropy Weight Water Quality Index (EWQI) method.

sample number	Aquifer name	EWQI price	Water quality classification
1	Second aquifer1st	85.2	Class III
2	Second aquifer2nd	72.3	Class III
3	Third aquifer1st	65.8	Class III
4	Fourth aquifer1st	90.1	Class III
5	Fourth aquifer2nd	88.5	Class III
6	Fourth aquifer3rd	102.3	Class IV
7	Fourth aquifer4th	78.9	Class III
8	Third aquifer2nd	115.6	Class IV
9	Third aquifer2nd	120.4	Class IV
10	Fourth aquifer	55.6	Class III
11	Third aquifer1st	45.2	Class II
12	Third aquifer3rd	48.9	Class II
13	Third aquifer4th	52.1	Class III
14	Third aquifer5th	60.3	Class III
15	Phreatic aquifer1st	40.8	Class II
16	Phreatic aquifer2nd	38.5	Class II
17	Second aquifer3rd	42.1	Class II
18	Second, third aquifer1st	50.2	Class III
19	Second, third aquifer2nd	53.6	Class III
20	Second, third aquifer3rd	58.9	Class III

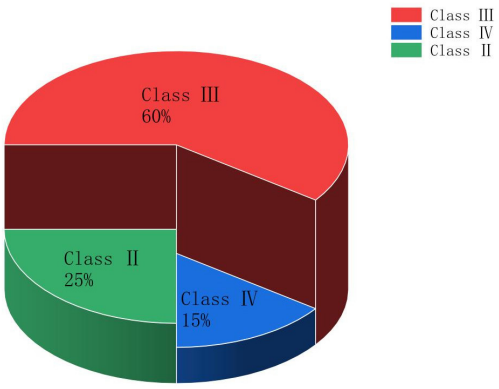

Fig. 6. Water type distribution in EWQI results.

200 mg/L for all samples, showing no non-compliance problems. The pH for most samples ranges between 8.0 and 8.9, characterizing them as weakly alkaline water [31], which meets the standards for domestic drinking water. The total hardness, calculated from Ca^{2+} and Mg^{2+}, is below 150 mg/L for all samples, categorizing it as soft water [32]. Based on the above data, it is inferred that the overall water quality across the aquifers in the study area is excellent, complying with Class I or II standards of the "Standard for Groundwater Quality". The results of the evaluation index selection method are shown in Fig. 5.

Principal Component Analysis

As presented in Table 3, the outcome of the Principal Component Analysis (PCA) method shows that PC1 (54.02%) is the total salinity factor, characterized by high-loading indicators including TDS, Cl^-, SO_4^{2-}, and K^++Na^+, indicating the degree of total mineralization

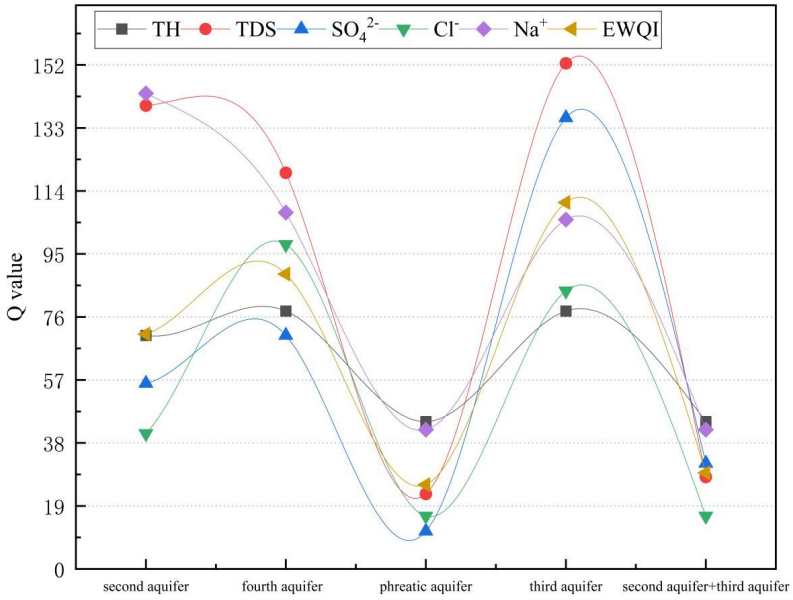

Fig. 7. Q-value distribution plot.

and the tendency towards salinization. PC2 (20.86%) constitutes the hardness and alkalinity factor, featuring high loadings on Ca^{2+}, Mg^{2+}, and HCO_3^- (inverse correlation), thereby illustrating the attributes related to water hardness and carbonate alkalinity. PC3 (12.71%) serves as the cationic composition factor, explained by high loadings on Ca^{2+} (positive) alongside Mg^{2+} and HCO_3^- (negative), indicating the relative ratio of the cations (calcium and magnesium). Based on the data model, it is inferred that the water from the fourth aquifer, parts of the third aquifer, and the phreatic aquifer constitute low mineralization zones [33]; most of the third aquifer and parts of the fourth aquifer represent medium mineralization zones; while parts of the second aquifer and parts of the fourth aquifer are high mineralization zones.

Entropy Weighted Water Quality Index

The results of the Entropy Weighted Water Quality Index (EWQI) method are presented in Table 4. The water type distribution based on EWQI classification is presented in Fig. 6.

Based on the tabulated data, Class II water comprises 5 samples (25%), corresponding to an EWQI range of 38.5-48.9; Class III water includes 12 samples (60%) with EWQIs from 50.2 to 102.3; and Class IV water consists of 3 samples (15%) having EWQIs between 102.3 and 120.4. The majority of samples (85%) fall into Class II or III, suggesting generally satisfactory overall water quality, yet the inferior quality at specific locations (e.g., third aquifer2nd) necessitates investigation into their pollution sources or geological impacts.

Contrastive Analysis

Variations in the fundamental principles of the three methodologies result in discrepancies in groundwater quality evaluation outcomes [34]. The evaluation indicator selection method fails to consider inter-indicator correlations; it cannot comprehensively reflect the overall water quality status and may mask anomalies in certain indicators. The interpretation of Principal Component Analysis (PCA) results relies on professional expertise; it does not directly correspond to water quality classes and is relatively sensitive to data distribution and sample size. In the EWQI method, the assignment of weights is solely based on data distribution, which risks neglecting significant yet low-variability parameters and remains susceptible to the influence of outliers. Therefore, selecting the evaluation results from the Entropy Weighted Water Quality Index method yields the optimal assessment outcome. This indicates that the phreatic aquifer water in the study region is in a fairly good state, where 85% of the samples attain Class II or III quality, and the other 15% fall into Class IV.

Quantitative comparison shows that the single-factor method classified 85% of samples as Class I or II for most parameters, but flagged SO_4^{2-} as a problematic parameter in 15% of samples. PCA highlighted that samples from the third aquifer have higher PC1 scores, indicating elevated mineralization. EWQI provided a more integrated classification, identifying 15% of samples (all from the third aquifer) as Class IV. The consistency among methods confirms that the third aquifer is the most impacted. The poor water quality in the third aquifer (Class IV samples) is likely influenced by coal mining activities: mine water drainage introduces high-salinity water, and coal gangue accumulation leaches

sulfate and other ions. Additionally, the third aquifer is closer to the coal seams, making it more susceptible to mining-induced fractures that enhance connectivity with contaminated zones.

Potential sources of uncertainty in this study include: (1) sampling limitations – only 20 samples collected during a single season may not capture temporal variability; (2) analytical errors – despite quality control, instrument precision and operator variability may introduce minor errors; (3) model assumptions – EWQI weighting depends solely on data distribution, which could overlook parameters with low variability but high health significance. Future work should incorporate repeated sampling across seasons and sensitivity analysis to quantify these uncertainties.

Conclusions

Utilizing 20 groundwater samples collected from the phreatic aquifer at the Xutuan Coal District, this research delves into the chemical properties and evolution patterns of the local groundwater through mathematical statistics, water type analysis, and traditional graphical methods, leading to three key findings. The shallow groundwater in Xutuan Coal District is slightly acidic freshwater, with hydrochemical type SO_4^{2-}·HCO_3^--Na^+·K^+. Water-rock interaction (evaporation, silicate weathering, cation exchange) dominates the chemical evolution, with coal mining activities (e.g., pyrite oxidation) contributing to elevated SO_4^{2-} in the third aquifer. EWQI reveals that 85% of samples are of good to moderate quality (Class II/III), while 15% (all from the third aquifer) are poor (Class IV), necessitating targeted monitoring and management. This multi-method approach provides a scientific basis for groundwater protection in coal mining areas.

Acknowledgements

This research was supported by the Anhui Provincial College Students' Innovation and Entrepreneurship Training Project (Grant No. S202510379072), the Open Fund of the Coal Industry Engineering Research Center for Exploration and Early Warning of Mine Water Disaster (Grant No. 2024-CIERC-07). The authors also acknowledge financial support from the Excellent Young Teachers Training Program of Anhui Province (Grant No. YQYB2024075), the Academic and Technical Leader Reserve Program of Suzhou University (Grant No. 2024XJHB08), and the Postdoctoral Research Startup Fund Project of Suzhou University (2025BSH001), and the Drilling Engineering Technology Research Center of Suzhou University (2024PT04). The authors also acknowledge additional financial support from the Anhui Provincial Department of Education Research Project (2023AH052224), the Anhui Provincial Department of Education Quality Engineering Projects (2024zygzts115; 2024jsqygz117), and the Suzhou University Institutional Quality Engineering Project (szxy2023xxhz01), which provided important assistance for the completion of this study. The authors acknowldege the Fund Project of National Engineering Research Center for Coal Mine Water Hazard Prevention and Control (WBMDGCZXJJ(2025)2); Innovation Team for Key Technologies of Co-extraction of Coal, Water and Heat (2024TDPY02).

AI Usage Disclosure Statement

During the preparation of this manuscript, the authors used DeepSeek (web version, V3) for language polishing, grammar checking, and expression refinement. After using this tool, the authors carefully reviewed and edited the content as needed and take full responsibility for the final version of the manuscript.

Conflict of Interest

The authors declare no conflict of interest.

References

1. ILMA A., RASHID U. Hydrogeochemical characterization and water quality assessment in parts of Indo-Gangetic Plain: An insight into the controlling processes. Sustainable Water Resources Management, **10**, 110, **2024**.
2. SONG K.C., HU H.Y., ZHANG H., GUAN S.Y., DENG W.H., YONG J.Y., ZHAO X.N., WANG X. Spatiotemporal niche separation mechanisms of water utilization strategies in the desert steppe plant communities, northern China. Journal of Arid Land, **17**, 1741, **2025**.
3. MHADHBI F., OLLIVIER G., NAPOLÉONE C. Exploring pathways to sustainable agriculture: Understanding institutional lock-in in Tunisia through analysis of stakeholders' discourse. Review of Agricultural, Food and Environmental Studies, **107,** 23, **2025**.
4. EID H.M., EISSA M., MOHAMED E.A., RAMADAN H.S., CZUPPON G., KOVÁCS A., SZŰCS P. Application of stable isotopes, mixing models, and K-means cluster analysis to detect recharge and salinity origins in Siwa Oasis, Egypt. Groundwater for Sustainable Development, **25**, 101124, **2024**.
5. DHEERAJ P.V., SINGH S.C., ALAM A., SONKAR A.K. Hydrogeochemical quality investigation of groundwater resource using multivariate statistical methods, water quality indices (WQIs), and health risk assessment in Korba Coalfield Region, India. Stochastic Environmental Research and Risk Assessment, **39**, 937, **2025**.
6. MARANDI A., SHAND P. Groundwater chemistry and the Gibbs Diagram. Applied Geochemistry, **97**, 209, **2018**.
7. DHAKATE R. Characterization of groundwater salinity by hydrogeochemical and multivariate statistical analysis in the coastal aquifer of Nagapattinam district, Southern India. Heliyon, **10** (11), e32396, **2024**.
8. YAN Y., SHI H., MIAO Q., ZHAO Y., NIE X., LI Z., PAN M., FENG W., GONÇALVES J.M., DUARTE I.M.

Evolution of chemical characteristics and irrigation suitability of groundwater in arid and semi-arid regions. Agricultural Water Management, **311**, 109361, **2025**.
9. PEQINI A., HEYDE B.J., BRAHUSHI F., DÜRING R.-A.Integrated analysis of the occurrence and in situ sediment-water partitioning of selected pharmaceuticals in a riverine system. Environmental Sciences Europe, **37**, 212, **2025**.
10. ZHOU Q., ZHANG J., ZHANG S., QIAN C., FAN H., CAO C., ZHANG Y., YANG Y., LUO J., YAO Y. Groundwater quality evolution across China. Nature Communications, **16** (1), 2522, **2023**.
11. FARAHMAND A., JAWADI H.A., ZARYAB A., HUSSAINI M.S., ALI S., ABRUNHOSA M., AZIZI F.R. Hydro-geochemical Assessment of Groundwater in a Semi-Arid Region of Western Afghanistan (Herat) Using the Entropy Water Quality Index (EWQI) and Multivariate Analysis. Water Conservation Science and Engineering, **10**, 136, **2025**.
12. DHEERAJ V.P., SINGH C.S., SONKAR A.K., KISHORE N. Heavy metal pollution indices estimation and principal component analysis to evaluate the groundwater quality for drinking purposes in coalfield region, India. Sustainable Water Resources Management, **10**, 31, **2024**.
13. SINGH B.P., CHOUDHURY M., SAMANTA P., GUPTA P. Hydrogeochemical Appraisal, Quality Assessment, Ecological and Human Health Risk Assessment in Groundwater of Hindon River Basin. Water Conservation Science and Engineering, **10**, 127, **2025**.
14. MOD K., HASIRCI G., HILMIOGLU N. Boron Removal from Water by Carbon Nanotube Loaded Biopolymer Sodium Alginate Adsorbent: Isotherm, Kinetic, Optimization Studies. Water, Air, & Soil Pollution, **237** (4), 248, **2026**.
15. WANG G., MAO H., CHEN X., ZHOU L., HUANG D., ZHANG F., YAN X. Spatial distribution and driving factors of groundwater chemistry and pollution in an oil production region in the Northwest China. Science of The Total Environment, **875**, 162635, **2023**.
16. RANA S., CHOUDHARY S., TIWARI S.K., YADAV J.S., SHARMA R. Source identification and geochemical characteristics of surface and groundwater from Larji-Rampur window, Himachal Himalaya: Implications for socio-environmental perspectives. Results in Earth Sciences, **3**, 100074, **2025**.
17. BIERNACKA A., BOJARCZUK A. Transformations in river water chemistry following wastewater treatment implementation in a mountain region of the Polish Carpathians. Environmental Science and Pollution Research, **32** (55), 30580, **2025**.
18. HONGWEI P., KAI B. Analysis of hydrochemical model and spatiotemporal differentiation characteristics of groundwater in the Handan-Xingtai area, China. Environmental Geochemistry and Health, **48**, 44, **2026**.
19. MENG Y., ZHANG Z.J., HAO Q.C., DONG Y., LI Y.S., WANG Z.X., CHENG C.X., ZHANG F.R., HAN P.F. The groundwater mixing mechanism and hydrogeochemical processes driven by coal mining in the typical area, Northern Ordos, China. Environmental Monitoring and Assessment, **198**, 41, **2026**.
20. AHMED S., MAZHAR M.A., HUSSAIN W. Spatial monitoring and analysis of haloacetic acids in drinking water using GIS: a case study of Jamia Nagar, New Delhi. Environmental Monitoring and Assessment, **198**, 46, **2026**.
21. ARVETI N. Hydrogeochemical characteristics and evaluation of groundwater quality in Varadaiahpalem, Andhra Pradesh, South India. Discover Environment, **3**, 264, **2025**.
22. WANG P., ZHANG W., ZHU Y., LIU Y., LI Y., CAO S., HAO Q., LIU S., KONG X., HAN Z., LI B. Evolution of groundwater hydrochemical characteristics and formation mechanism during groundwater recharge: A case study in the Hutuo River alluvial-pluvial fan, North China Plain. Science of The Total Environment, **915**, 170159, **2024**.
23. ZAHI F., DROUICHE A., AZZEDDINE R., MEDJANI F., DJIDEL M. Hydrogeochemical processes controlling surface water quality for irrigation in a Mediterranean wetland ecosystem, Northeast Algeria. Environmental Monitoring and Assessment, **196**, 881, **2024**.
24. REYES-TOSCANO C.A., CORTÉS-MARTÍNEZ R., ALFARO-CUEVAS-VILLANUEVA R., VÁZQUEZ-MEJÍA G., FONSECA-MONTES-DE-OCA R.M.G., FUENTES-RIVAS R.M., ZANOR G.A. Hydrogeochemical analysis and water quality assessment of the Duero River in an agricultural region of Mexico. Environmental Geochemistry and Health, **48**, 43, **2026**.
25. TRAN T.Q., WOHNLICH S., RIECHELMANN S., BANNING A. Environmental relevance monitoring and assessment of ochreous precipitates, hydrochemistry and water sources from abandoned coal mine drainage. Environmental Monitoring and Assessment, **196**, 700, **2024**.
26. CHEN J.Q., WANG Z., LIU H.Y., YANG Y., ADIMALLA N., LI Y.G., ZHI C.S., WANG B. Formation mechanism and health risk assessment of high fluoride geothermal water in Gonghe Basin, Northwest China. Environmental Geochemistry and Health, **47**, 572, **2025**.
27. DAS A. Surface water quality evaluation impacting drinking water sources and sanitation using water quality index, multivariate techniques, and interpretable machine learning models in Mahanadi River, Odisha (India). Environmental Geochemistry and Health, **47**, 497, **2025**.
28. OBRIKE S.E., SALEH A.I., ANUDU G.K., MAGAJI I.A., IYAKWARI S. Hydro-geochemical evolution, quality, and health risk assessment of groundwater in crystalline basement aquifer in Keffi, Nigeria. International Journal of Energy and Water Resources, **9**, 727, **2025**.
29. HUANG X.J., WANG G.C., XIE Z.D., ZHAO Y.B., OU L., JIANG C. Unraveling the hydrogeochemical characteristics and pollution sources of groundwater in an intensive industrial area, East China. Environmental Science and Pollution Research, **31**, 50179, **2024**.
30. YAN H., ZHANG P., HAN B. Concentrations, Sources and Health Risk of Boron in Surface Water of Huaihe River Basin, China. Water, Air, & Soil Pollution, **236**, 910, **2025**.
31. PANT R.R., KHANAL B., ACHARYA A., POUDEL P., BOHARA R., AWASTHI M.P., PARAJULI S., CHAND M.B., BISHWAKARMA K., KANDEL K., THAKUR T.K. Hydrochemical characteristics and water quality assessment of surface water in the Badigad River Basin, Lesser Himalayas, Nepal. Environmental Science and Pollution Research, **32**, 19836, **2025**.
32. PANG K., REN Z.Y., LUO K.L., HAO L.T., YANG S.J. Hydrochemical characteristics and water quality assessment of natural water in the South China Mountains: the case in Lianzhou. Environmental Geochemistry and Health, **45**, 9837, **2023**.
33. KHOUNI M., CHAABANE H., GRÜNBERGER O., NEGRO S., HAMMECKER C. Adsorption and mineralization of metalaxyl-m and chlorpyrifos in

irrigated Mediterranean soil under the effects of salinity. Environmental Science and Pollution Research, **31**, 63016, **2024**.

34. QIANG Y.C., LU S., XIE Y.Q., XIE Z.J., ZHU M.J. A comparative assessment of groundwater and surface water quality in the Yangtze River Delta. Environmental Monitoring and Assessment, **197**, 729, **2025**.
35. EID M., AWAD M., MOHAMED E., NASSAR T., ABUKHADRA M., EL-SHERBEENY A., KOVÁCS A., SZŰCS P. Comprehensive approach integrating water quality index and toxic element analysis for environmental and health risk assessment enhanced by simulation techniques. Environmental Geochemistry and Health, **46**, 409, **2024**.